

Winfried Herrmann

**Confinement of ripple-trapped
slowing-down ions by a
radial electric field**

CONFINEMENT OF RIPPLE-TRAPPED SLOWING-DOWN IONS BY A RADIAL ELECTRIC FIELD

Winfried Herrmann and the ASDEX Upgrade Team

Max-Planck-Institut für Plasmaphysik

EURATOM-Association

D-85748 Garching

Abstract

Weakly collisional ions trapped in the toroidal field ripples at the outer plasma edge can be prevented to escape the plasma due to grad B-drift by a counteracting radial electric field. This leads to an increase in the density of ripple-trapped ions, which can be monitored by the analysis of charge exchange neutrals. The minimum radial electric field E_r necessary to confine ions with energy E and charge q ($q=-1$: charge of the electron) is $E_r = -E/(q * R)$, where R is the major radius at the measuring point. Slowing-down ions from neutral injection are usually in the right energy range to be sufficiently collisionless in the plasma edge and show the confinement by radial electric fields in the range of tens of kV/m. The density of banana ions is almost unaffected by the radial electric field. Neither in L/H- nor in H/L-transitions does the density of ripple-trapped ions and, hence, the neutral particle fluxes, show jumps in times shorter than 1 ms. According to [1,2] the response time of the density and the fluxes to a sudden jump in the radial electric field is less than 200 μ s, if the halfwidth of the electric field is larger or about 2 cm. This would exclude rapid jumps in the radial electric field at the transition. Whether the halfwidth of the electric field is that large during transition cannot be decided from the measurement of the fluxes alone.

1. Introduction

Shear in a radial electric field and, connected with it, shear in the $E \times B$ -flow is almost unanimously believed to cause improvement in plasma confinement in the plasma interior as well as in its edge by the suppression of fluctuation-driven enhanced transport. For a comprehensive study of the literature see [3]. Especially a radial electric field in the plasma edge, close to the separatrix, is considered to generate the very beneficial improvement in confinement in the H-mode (high confinement mode). The theoretical understanding of the processes involved in the transition from L-mode (low confinement mode) to H-mode must be related to and based on measurements of fluctuations and the radial electric field. Measurements of radial electric field in the plasma turn out to be very demanding, if results with good time and, simultaneously, good spatial resolution are required. Heavy ion beams are not installed at larger plasma experiments because of the excessive acceleration energy necessary. The molecular beam [4], which should be well suited especially for application at the plasma edge, has not yet been applied. The same is true for a new method using the motional Stark effect [5]. The most direct result could be obtained by movable emitting probes [6]. Their application, however, is limited to low energy plasmas because of possible damage to the probes and their influence on the plasma. The method used widely up to now is therefore a rather indirect method of inferring the radial electric field from the radial force balance in the plasma:

$$E_r = \frac{1}{en_i Z_i} \nabla_r p_i + [v \times B]_r$$

This involves the measurement of radial profiles of density and temperature of one ion species as well as the measurement of its mean poloidal and toroidal rotation velocity. All this information can usually be obtained from measurements of charge exchange resonance spectroscopy. The main disadvantage of this type of measurement is the up to now poor time resolution. One of the results of such measurements [7] is, that, at least for times not too close to the transition, the main contribution to the radial electric field at the plasma edge is from the pressure gradient. Whether this is true also at and shortly after the L/H-transition is still unknown because of the poor time resolution of the velocity measurement. Which force creates the electric field and drives the strongly damped rotation connected with it is still an important topic of discussion and controversy. The problem arises when the electric field jumps at the transition and the pressure gradient can not follow to compensate the poloidal rotation.

This paper will not be able to solve this problem, but it may contribute to

the understanding of the time behaviour of the radial electric field at the L/H-transition and during ELMs.

The paper describes a novel method, that allows one to measure aspects of the radial electric field at the plasma edge, especially its time behaviour, with a time resolution of about $100 \mu\text{s}$. A few results obtained with this new method have been published earlier [8]. They can be summarised by the statement, that a radial electric field with more than about 5 kV/m could not be detected before the L/H-transition, and that after the onset of the transition the field grows to not more than about 10 kV/m in 1 to 2 ms. The further growth of the field to 20 kV/m or, as shown in this paper, to more than 40 kV/m may need times longer than 100 ms. The present paper will confirm these earlier observations, but add some conditions that should be fulfilled to really exclude rapid jumps of the field at the transition.

In this new method the information about the electric field comes from the measurement of the density of weakly collisional ripple-trapped ions in the plasma edge which, without a radial electric field, is rather low, because of the rapid loss of such ions due to the gradB-drift. As is well known [3], radial electric fields in the plasma edge can have a strong effect on confinement of ripple-trapped ions, when the $E \times B$ -drift is opposite but of about the same magnitude as or larger than the grad B-drift. Ions that are otherwise lost rapidly can be well confined under these circumstances, and the density of these ions is enhanced in the plasma edge. This can be detected by neutral particle analysis. As thermal ions in the plasma edge are of low energy and hence their collision frequency can exceed the ripple trapping rate, their confinement is only weakly improved by the electric field. Of much larger benefit are here the energetic slowing-down ions from neutral injection, that are present in the plasma edge as well as in the interior. The discrimination of neutrals stemming from charge exchange at the edge from those from the interior is made easy by the strong decrease of the neutral density, as one moves radially inward, with the result that neutral fluxes are dominated by charge exchange processes near the edge.

The paper is organized as follows: Chapter 2 describes the experimental setup, including the geometry of ASDEX Upgrade and of the charge exchange analyzers. Furthermore information about the toroidal ripple and its effective value for a specific q-profile, the deposition profiles of the heating beams and typical banana orbits of injected ions, and an example of a neutral density profile are included. In chapter 3 a relation between maximum field strength for a given halfwidth of the field and the energy of ions that can be confined will be established. It will also be demonstrated that a fast reaction of the fluxes to a sudden increase of

an electric field is possible and the more effective, the larger the halfwidth of the field. Chapter 4 contains the experimental results. After a demonstration of the principal effect, it is shown how a rough measure of the electric field strength can be obtained and how this relates to the pressure gradient. Finally, the time behaviour at the L/H-transition is discussed, based on a few examples where an L/H- and an H/L-transition has been observed with good time resolution. A summary concludes the paper.

2. Experimental Setup

The experimental technique of the electric field measurement relies on the measurement of the density of ions that are trapped in the ripples of the toroidal magnetic field due to the finite width of the toroidal field coils. These ions execute charge exchange collisions with background neutrals and can escape the plasma as neutrals. These can be detected using neutral particle analyzers with energy, mass and time resolution [9]. The electric field can change the density of only nearly collisionless ions, as only those have a chance to escape the plasma as ions due to the gradB-drift and, hence, reduce the density of ripple-trapped ions in the absence of an electric field. Slowing-down ions from neutral injection have low enough collisionality as long as their energy is larger than a few keV, depending on plasma conditions. As the scattering time is usually much longer than the slowing-down time, the population of ripple-trapped fast ions decreases with more parallel injection of the beams. A poloidal and toroidal cross-section of ASDEX Upgrade is seen in Figure 1. The positive toroidal and poloidal directions are anticlockwise and downwards at the outside. Two neutral particle analyzers are installed at ASDEX Upgrade. The figure shows the viewing line of one fixed position analyzer and the pivot point with the range of viewing lines for the movable analyzer. The fixed analyzer views the plasma almost radially. The local pitch angle $\xi = \arctg(v_{\parallel}/v_{\perp})$ of the neutrals seen depends weakly on the safety factor q_{95} and ranges between $\xi = 1.3^{\circ}$ for $q_{95} = 3$ and $\xi = 1.1^{\circ}$ for $q_{95} = 5.7$. Ions with $\xi > 5.7^{\circ}$ close to the separatrix are on banana orbits. The fixed analyzer, therefore, views deeply trapped ions. The movable analyzer can be set to view deeply ripple-trapped ions as well as banana ions, depending on its poloidal and toroidal viewing angle. All data for this paper have been taken with a poloidal angle of 15° , directed towards the plasma center. For $q_{95} = 4$ the following local ξ -values for toroidal angles α and observation points close to the separatrix are obtained:

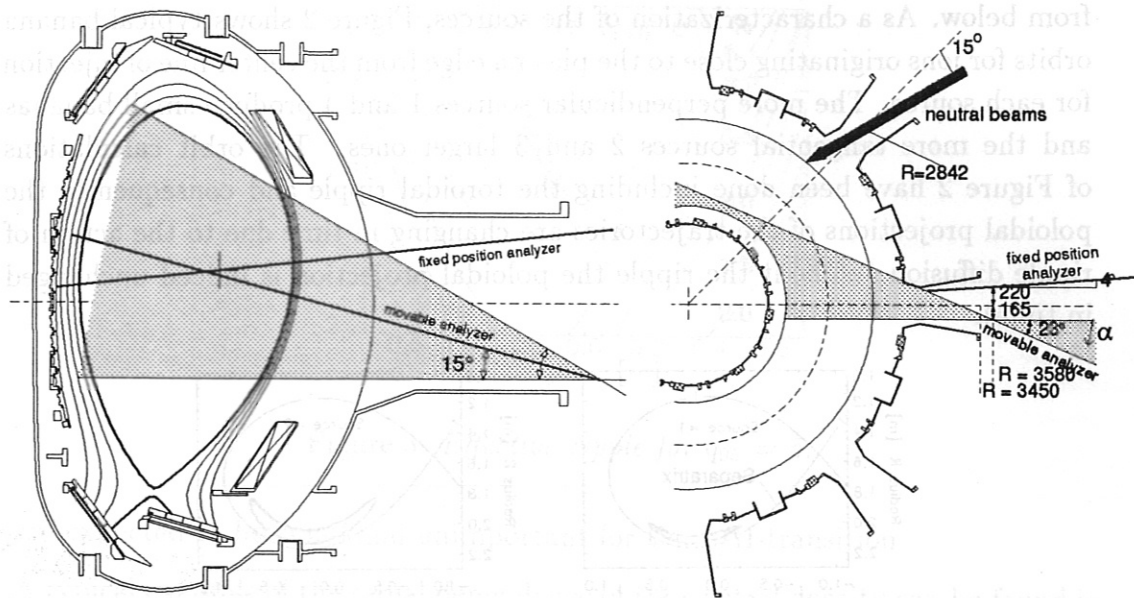


Figure 1: left: *Poloidal cross-section of ASDEX Upgrade with neutral particle analyzer viewing lines*; right: *top view of the midplane of ASDEX Upgrade*.

α [°]	ξ [°]	status
0	-3.8	banana
3	1.0	ripple
6	6.0	banana
9	11.0	banana
12	16.0	banana

For $\alpha > 5.5^\circ$ the analyzer observes banana orbits of ions, if they are close to the separatrix.

The maximal count rate of the detectors in the analyzers is slightly more than 10^6 pulses per second. The maximum time resolution with acceptable signal to noise ratio is therefore about $100 \mu\text{s}$. Usually, however, the sampling time, which is the same for all energy channels of the analyzer, is set to larger values, to avoid excessive statistical errors in energy channels with small fluxes only.

The mean line of injection for the four sources of neutral injection lies in the horizontal midplane with a toroidal angle of 15° at the radius of $R = 2.842 \text{ m}$. Two beams inject more tangential (toroidal angle 26° at the separatrix), two more perpendicular (toroidal angle 14.5°); two beams inject from above and two

from below. As a characterization of the sources, Figure 2 shows typical banana orbits for ions originating close to the plasma edge from the center line of injection for each source. The more perpendicular sources 1 and 4 produce small bananas and the more tangential sources 2 and 3 larger ones. The orbit calculations of Figure 2 have been done including the toroidal ripple and consequently the poloidal projections of the trajectories are changing in time due to the action of ripple diffusion (without the ripple the poloidal projection is indeed unchanged in time).

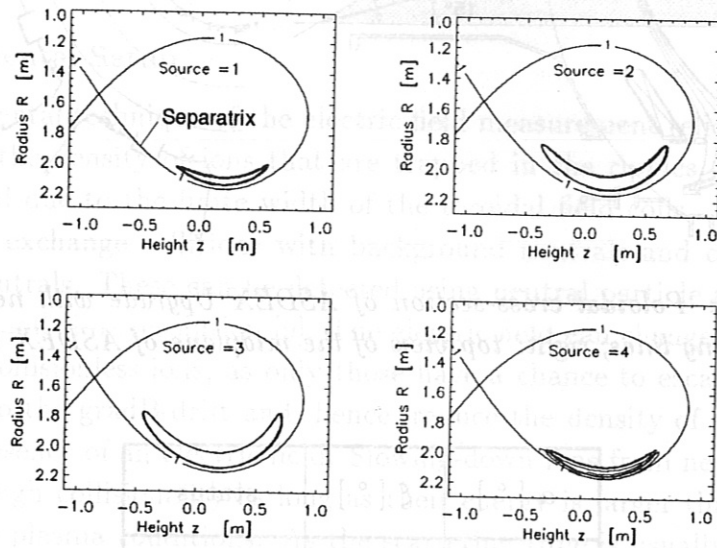


Figure 2: Gyro-orbits for central ions of the ASDEX Upgrade beam sources.

The toroidal field ripple in ASDEX Upgrade is symmetric across the geometrical midplane of the toroidal field coils but, because of the vertical shift of the plasma, the ripple at the separatrix is larger at the upper half of the plasma than on the lower half. However, important for the trapping of the ions is not the toroidal ripple, but the ripple seen by the ion along its drift trajectory. This effective ripple is plotted in Figure 3 for a discharge with $q_{95} = 5$; effective ripple is defined as the ripple along a field line between two coils, assuming that the drift orbit does not deviate too much from field lines for short toroidal distances. The toroidal field ripple has been used in a parameterized form [10] fitted to values calculated from the coil currents.

With a negative toroidal field, ripple-trapped ions drift downward and, for certain large radii, hit regions without effective ripple, become detrapped and confined as banana ions. With positive toroidal field and drift upward, banana ions may become trapped and lost from the plasma. These inward and outward currents

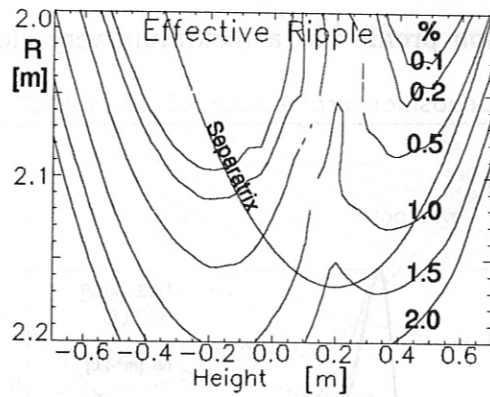


Figure 3: *Effective ripple for $q_{95} = 5$.*

are expected to be small and unimportant for the L/H-transition.

A typical example of the radial dependence of the neutral density can be found in Figure 4. This figure has been obtained from Monte Carlo calculations [11] with

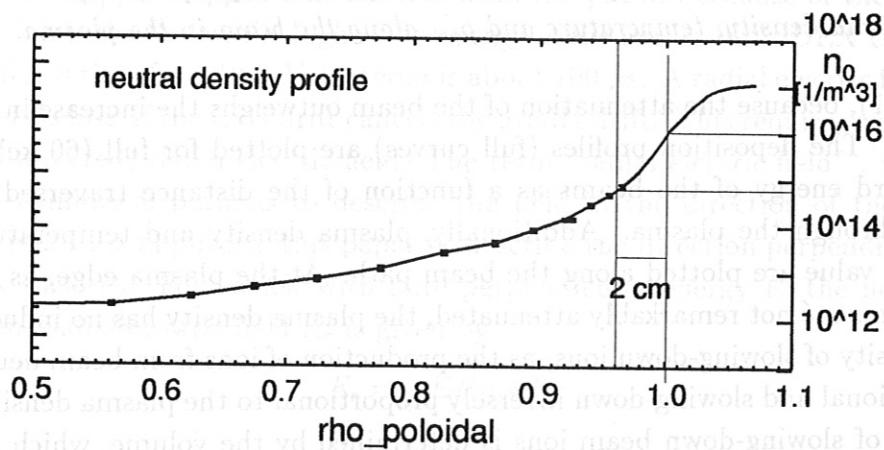


Figure 4: *An example of the neutral density profile for an H-mode plasma density profile (#8252 at $t=3.868$ s).*

the code EIRENE [12] using optimized ion temperature profiles to fit the fluxes measured with the neutral particle analyzer. It is important to note that the neutral background density from the wall sources decays rapidly radially inward with the result that the largest fraction of a neutral particle flux originates from a region close to the plasma edge, if the source distribution of the fast ions is constant.

An example of the deposition of injected beam neutrals is given in Figure 5 for an H-mode density profile (a combined result from interferometry and Li

beam). The deposition profile has a maximum very close to the plasma edge

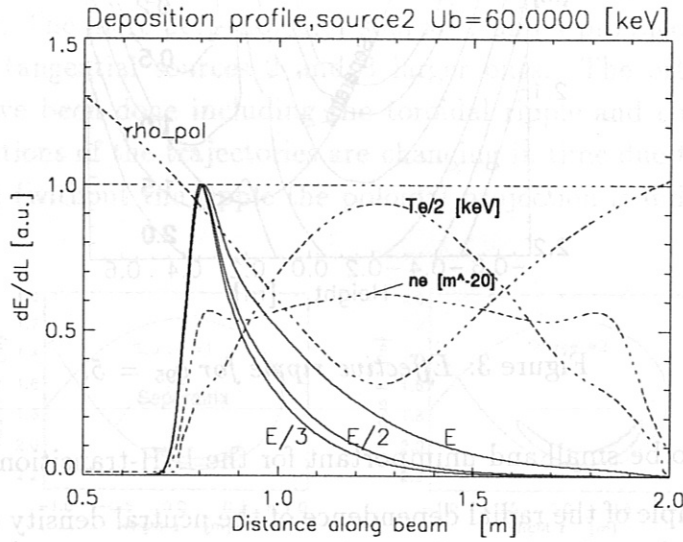


Figure 5: Power deposition for a central ion of source 2 for full, half, third energy and plasma density, temperature and ρ_{pol} along the beam in the plasma.

($\rho_{pol} = 1$), because the attenuation of the beam outweighs the increase in plasma density. The deposition profiles (full curves) are plotted for full (60 keV), half and third energy of the beams as a function of the distance traversed by the beam through the plasma. Additionally, plasma density and temperature and the ρ_{pol} value are plotted along the beam path. At the plasma edge, as long as the beams are not remarkably attenuated, the plasma density has no influence on the density of slowing-down ions, as the production of ions from beam neutrals is proportional and slowing-down inversely proportional to the plasma density. The density of slowing-down beam ions is determined by the volume, which is filled by the slowing-down ions and - more important - by the electron temperature that influences the slowing-down rate, but the production rate only very little. From Figure 6, which has been obtained following [13], it can be seen, that the slowing-down density increases only slightly faster (proportional to $T_e^{1.5}$) than the electron temperature. This increase, however, is probably not enough to compensate the decay of the neutral density. The neutral flux, therefore, will originate predominantly from a region close to the separatrix, where a radial electric field is established during H-mode.

3. Necessary Field Strength for Confinement and Single Ion Trajectory Analysis

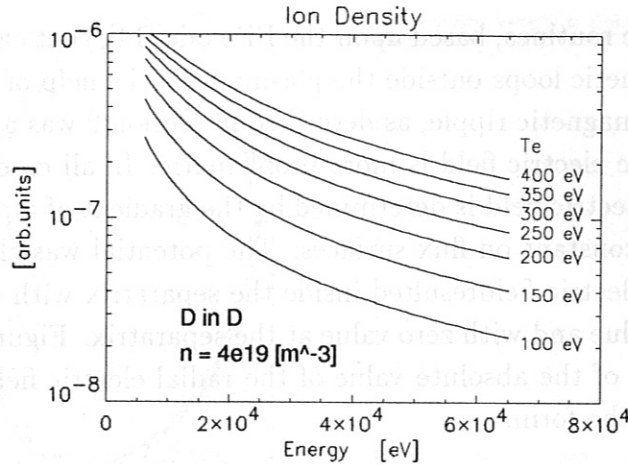


Figure 6: *Density of slowing-down ions as a function of ion energy and for different plasma temperatures.*

3.1 Minimum radial electric field for confinement

Collisionless ripple-trapped ions are lost from the plasma because of the gradB-drift, which is the faster, the higher the energy of the ion is. In ASDEX Upgrade, a typical loss time for a 10 keV deuteron is about $100 \mu s$. A radial electric field can prevent this loss, if the ExB-drift cancels the gradB-drift. This requires a negative (inward directed) radial electric field. The term “radial electric field”, which is used in cylindrical plasmas to describe the field in the direction of the minor plasma radius, is applied in this paper to describe the direction perpendicular to the flux surfaces. For an ion with pure perpendicular energy E , the necessary minimum radial electric field E_r is given by

$$E_r = -E/(q * R)$$

At the outer edge of the plasma with a large radius $R \approx 2$ m the relation indicates that a field of -5 kV/m could suffice to confine a 10 keV ion with $q = 1$ ($-q$ is the charge in electron units). Note that the mass and the magnetic field do not appear in the relation. As the two drifts are usually not exactly opposite to each other and the radial electric field is not homogeneous, a relation $E_{rm}[kV/m] \approx E[keV]$ has been used for an estimate of the maximum absolute value of a radial electric field with a peak close to the separatrix. Single ion trajectory calculations for ASDEX Upgrade geometry confirm this relation between field and energy of confined ions as long as the halfwidth of the field is in the range of a few cm (see Figures 10 and 11).

3.2 Choice of the fields for ion trajectory calculations

The magnetic field for the trajectory calculations has been taken from standard

ASDEX Upgrade routines, based upon the FP-code [14], that calculates magnetic fluxes from magnetic loops outside the plasma with the help of function parameterization. The magnetic ripple, as described in section 2 was added to this field. The choice of the electric field is more problematic. In all cases it was assumed that the radial electric field is determined by the gradient of a potential and that the potential is constant on flux surfaces. The potential was chosen such that a negative radial electric field resulted inside the separatrix with desired halfwidth and minimum value and with zero value at the separatrix. Figure 7 shows a three dimensional plot of the absolute value of the radial electric field, obtained from a potential U of the form:

$$U = k \cdot \exp(-(\rho_{pol} - 1)/r_e)^2.$$

For the plot the values of the radial electric field outside the separatrix have

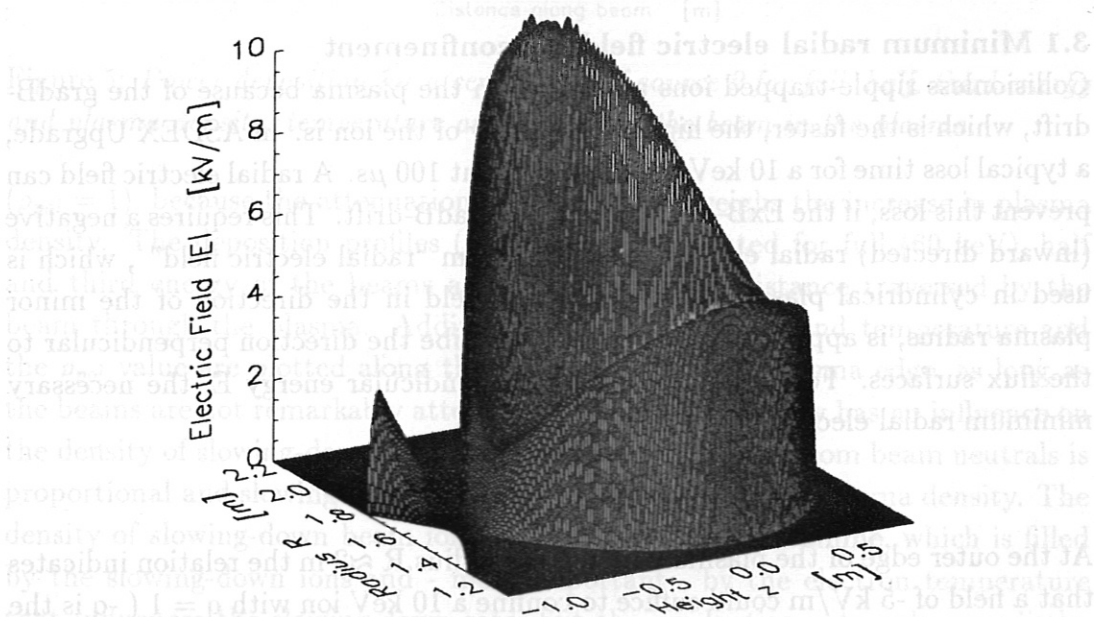


Figure 7: Absolute value of the electric field according to a Gaussian potential profile on flux surfaces; only values inside the separatrix are shown.

been omitted, and a rather large halfwidth of $r_e = 6$ cm has been used for clarity. The field is perpendicular to the flux surfaces and directed towards the plasma interior. Because of Shafranov shift, the flux surfaces are closer together at the low field side of the plasma, and the radial electric field is therefore higher at the low field side than at the high field side. The fields get very small in the neighbourhood of the X-point and at the top of the plasma, because of the large separation of the flux surfaces in these regions.

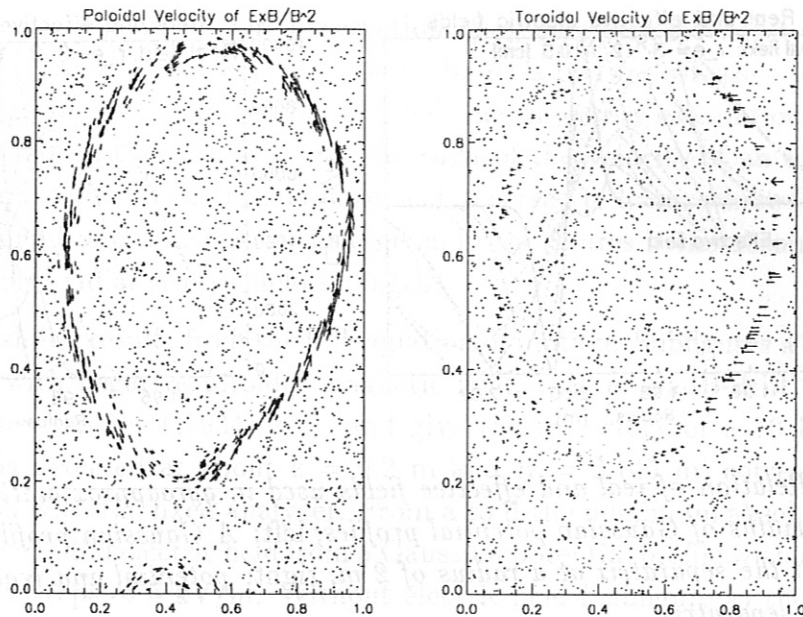


Figure 8: *Poloidal and toroidal $E \times B$ -velocities for a real magnetic configuration of ASDEX Upgrade and the electric field of Figure 7.*

Figure 8 gives an impression of the poloidal and toroidal velocities caused by the radial electric field in the magnetic field. The variation in velocity on a flux surface is even larger than the variation in radial electric field because of the decay of the magnetic field with radius. This strong velocity dependence should be very important for the calculation of poloidal damping.

If the halfwidth of the radial electric field is only a few cm, it is in the range of the Larmor diameter of the observed fast beam ions. Under such circumstances the gyroapproximation has to be used with great care for the orbit calculations. On Figure 9, real fields from a Gaussian potential profile with different decay lengths are compared with the effective field that, in gyroapproximation, would cause the same $E \times B$ -drift for a 10 keV deuteron in a constant toroidal magnetic field of 2 T. The curves reaching the maximal value of 10 kV/m represent the real field, the other curves give the effective field. The different line styles are for $r_e = 0.5/1.0/2.0/3.0$ cm in the Gaussian potential profile with full/dotted/dashed/dash-dotted line correspondingly. The separatrix, where the electric field is zero, has been set to 2 m. Fields on this plot are positive inside the separatrix. The differences between the real and the effective fields are most severe, as expected, for small r_e , with a strong reduction in maximum amplitude and a radial shift of the maximum. The halfwidth is not affected that much. However, if the field outside the separatrix is assumed to be much smaller than

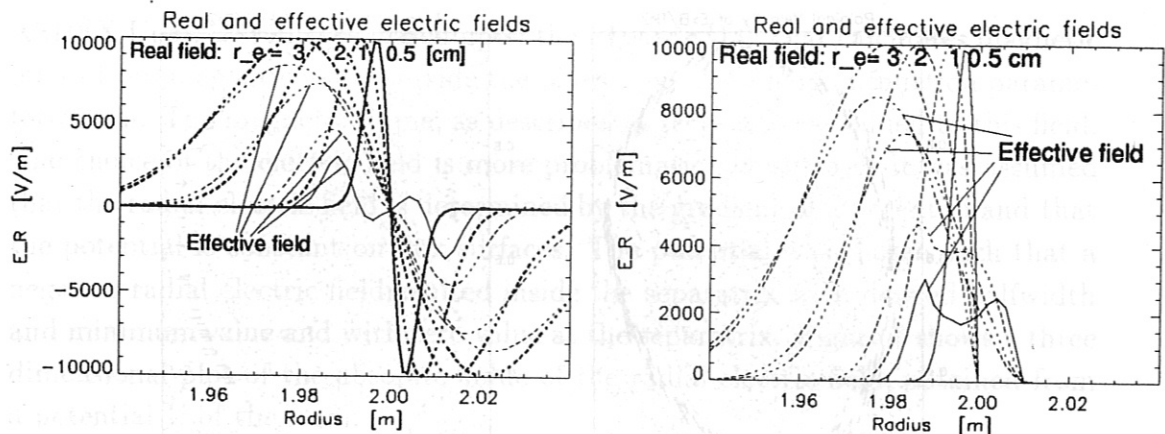


Figure 9: Relation of real and effective fields used in gyroapproximation for different halfwidths of Gaussian potential profiles; left: A Gaussian profile with real field zero at the separatrix at a radius of 2 m; right: potential and real field zero outside the separatrix.

inside or even zero, then the effective field stays finite outside the separatrix for the extent of one Larmor radius (see right plot of Figure 9).

The effective field is not constant during the slowing-down process of the ion. The gyroapproximation in its simple form should be restricted to fields with a halfwidth larger than the Larmor radius of the fast ion. For fields with smaller halfwidth a more complicated treatment of the electric field profile will be necessary in the trajectory calculations.

3.3 Single particle trajectory calculations.

Single particle trajectory calculations have been done using full equations of motion and gyroapproximation. Figure 10 and Figure 11 show a few examples of results. Of special interest in the context of this paper is the trajectory of an ion before charge exchange and detection by the analyzer. If the ion has a trajectory, that originates outside the plasma and spends only a short time inside the plasma, its trajectory should be almost empty, as there is no source outside the plasma and time is too short for ions on neighbouring trajectories to scatter into the observed trajectory inside the plasma. If the trajectory is confined in the plasma, it will be filled with ions according to the sinks and sources (mainly scattering) on this trajectory. Because of the asymmetry of the effective ripple (see Figure 3) this is not equivalent to the problem, whether an observed ion was on a loss orbit or a confined orbit; a trajectory, starting outside the plasma, may become confined after passing the observation point and may finally be well filled, but not at the time of observation; and vice versa: a trajectory, that was

confined for a long time before observation, may become a loss orbit (due to ripple diffusion) after the observation point. To get a picture, whether the observed trajectories would be rather empty or filled, the trajectory calculations have been done therefore in the reverse mode: the sign of the velocity of an observed ion and the sign of the magnetic field have been reversed to learn, where the detected ion is coming from. The electric field given in the figures is the absolute value of the minimum radial electric field strength.

Figure 10 shows results from the full equation of motion. Subfigures a to d belong to a case with negative toroidal magnetic field, that is gradB-drift downwards towards the X-point (#7934, 2 s), and give the trajectory of a 10 keV proton before it is detected at about $z = 0.2$ m and $R = 2.145$ m, corresponding to observation with the fixed analyzer. From a to d the maximum absolute value of the negative radial electric field from a Gaussian potential profile with $r_e = 3.0$ cm increases in steps of 5 kV/m. Without electric field (subfigure a) the trajectory - interpreted now in forward direction - originates outside the separatrix and spends only about 100 μ s inside the plasma. Due to gradB-drift the ion on such a trajectory moves downward. With a maximum absolute value of the negative electric field of 5 kV/m (subfigure b) the trajectory is not yet changed very much, it still originates outside the plasma. (Details in the trajectory result from aliasing effects, because of plotting only a fraction of the calculated points.) Because of the compensating action of the ExB-drift the ion spends longer time in the plasma but moves a bit radially because of the uncompensated radial component of the ExB-drift.

A value of 10 kV/m suffices to fully compensate the gradB-drift. As the ExB-drift is nearly vertical in this part of the plasma, the trajectory is confined to a rather small volume. No large changes appear, when the field is further increased to 15 kV/m. The trajectory remains ripple-trapped, but confined.

Subfigures e to h give trajectories for a positive toroidal magnetic field and gradB-drift upwards, away from the X-point (#8595, 2 s). The radial electric field is again given by a Gaussian potential profile with $r_e = 2.5$ cm and the field is zero outside the separatrix and its minimum value is fixed at -12.5 kV/m. From e to h the observation point at $z \approx 0.2$ m moves inward in steps of 0.5 cm. For the observation point close to the separatrix (e) the trajectory of a 10 keV deuteron starts outside the plasma and moves upwards with the gradB-drift. The ExB-drift according to the average radial electric field seen by the ion, slows down the upward drift, but is not able to fully compensate the gradB-drift. In subfigure f, with the observation point 0.5 cm further inward, the average electric field is strong enough to overcompensate the gradB-drift at the observation point.

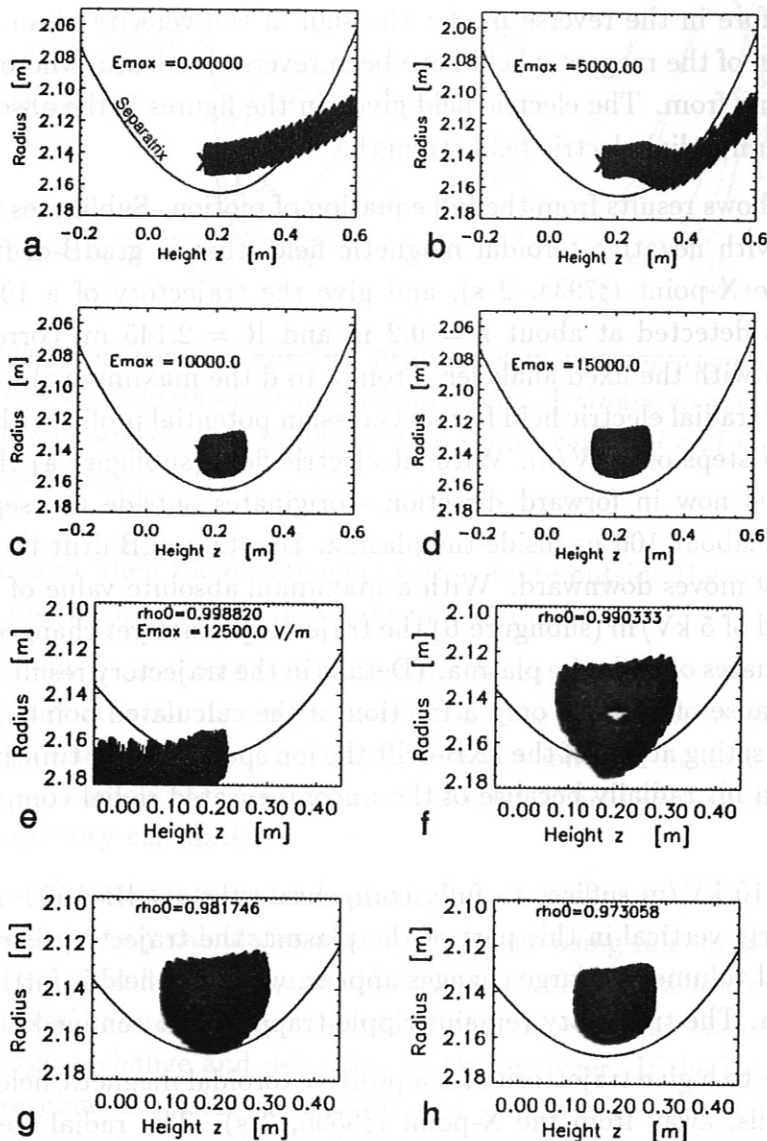


Figure 10: Ion orbits before seen by the analyzer via charge exchange for different maximal absolute values of the negative electric field (a to d) and different positions of observation (e to h). a to d are for 10 keV protons with $r_e = 3$ cm in a negative magnetic field; e to h for 10 keV deuterons with $r_e = 2.5$ cm in a positive magnetic field.

Because of the curvature of the flux surface the ExB-drift has an outward directed component, which cannot be compensated by the gradB-drift and in the reverse mode the ion therefore moves up- and inward, crosses the region of the electric field and then drifts downward according to the reversed gradB-drift, until it feels the electric field again and starts to move up- and outward to form a closed trajectory. The ion stays ripple-trapped all the time, but performs a closed orbit. The observation point is rather close to the separatrix, where the neutral density is large. It may be, that this type of orbit dominates the measured neutral flux. The electric field in this case connects regions from further inside the plasma, where the slowing-down ion density is larger because of the higher plasma temperature, to the outside, where the detection probability is larger. This way the electric field leads to an increase in the measured fluxes in times necessary for an ion to drift from the inner side to the outside, which is less than $100 \mu\text{s}$. The effect is enlarged, as the ripple further inside the plasma and hence the scattering time from well filled banana orbits to this trajectory is smaller than further outside. These may be the main contributions to the fast response of the flux to the radial electric field. For further discussions on this topic see References [1,2], where the rapid response of the fluxes to the field are explained and demonstrated in Monte Carlo simulations and Fokker-Planck calculations.

With observation points further inward (g and h) the orbit remains confined with smaller radial extent and less effect on the flux. For detection points even further inward, orbits similar to the one in subfigure f will be obtained that do not, however, contribute significantly to the flux, because of the low neutral density there.

Figure 11 has been produced using gyroapproximation in the trajectory calculation. The observation point in the reverse calculation (#7934, 1.9 s, negative toroidal magnetic field and drift downward to the X-point) is marked by a large cross. It corresponds to an observation point by the movable analyzer and has a position, where the ExB-drift already has a non-negligible component in the direction of the major radius, that cannot be compensated by the gradB-drift. The halfwidth r_e in the Gaussian potential profile has been chosen in this case to be 3 cm, to simulate a real field with a real r_e of about 2.5 cm. With a starting point close to the separatrix a negative field with a maximum absolute value of 5 kV/m brings ions from significantly further inward to the observation point. This effect is even larger at 10 kV/m. With 15 kV/m a new effect appears: Banana ion orbits that are almost not influenced by the radial electric field but may be well filled can become ripple trapped because of ripple diffusion and be brought to the observation point by the radial electric field. This effect may be yet an-

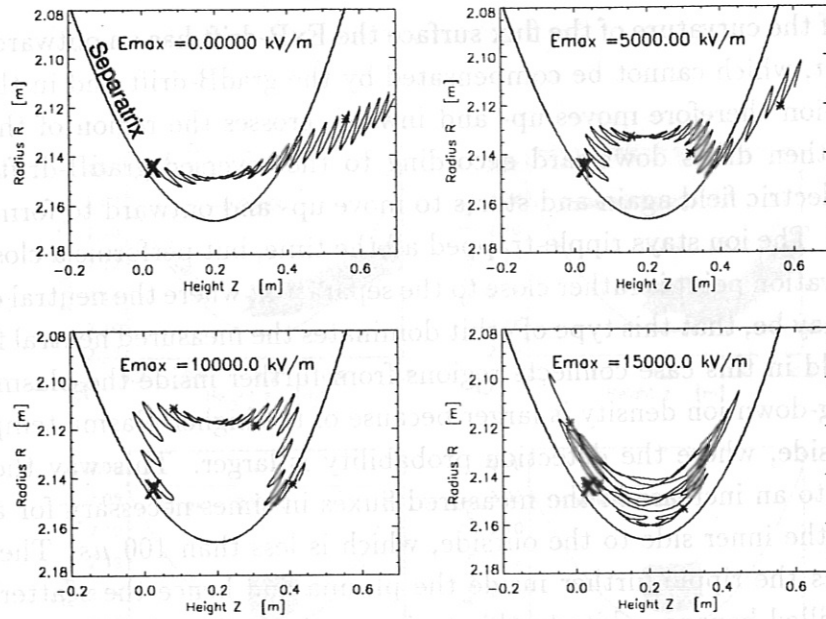


Figure 11: *Gyro-orbits of 10 keV deuterons before charge exchange at X to neutrals, that hit the analyzer. E_{max} is the maximum field strength of the absolute value of the negative electric field.*

other reason for the fast response of the neutral fluxes to a radial electric field. It, however, may be restricted to observation from below the magnetic midplane.

The estimate of the electric field from the rule of fist, that a -10 kV/m field can confine 10 keV deuterons, is applied to measurements with the fixed analyzer only that observes neutral fluxes from regions close to the magnetic midplane. Many calculations have shown, that this relation is applicable for halfwidth of a Gaussian potential profile larger or about 3 cm. The fields necessary for confinement will increase with a reduction of r_e , following the relation of effective field and real field of Figure 9. The possibility for the fast response of the neutral fluxes to the electric field by moving inner trajectories to the outside remains also at smaller r_e . This is also be the reason, why fluxes, measured by the movable analyzer from below the midplane, increase already at field strengths that are not yet sufficient to confine ripple-trapped ions.

4. Experimental Results

As has been shown earlier [8] and as can be seen in Figures 16 to 20, the flux of energetic ripple-trapped ions increases, when the plasma transits from L-mode to

H-mode. This is interpreted as the consequence of a growing radial electric field. The larger the field, the higher the energy of the fluxes that show an increase. In this section it is shown that this flux increase is indeed limited to ripple-trapped ions and banana ions are almost unaffected. This is also true for the effect of ELMs. For selected times the estimate of the radial electric field, obtained from the energy of the fluxes that are influenced by the field, is compared with the electric field resulting from the pressure gradient. The second topic of this section will concentrate on the time behaviour of the fluxes and on the question, whether a limit on the growth rate of the electric field can be obtained from the flux measurements.

4.1 Flux spectra for Banana- and Ripple-trapped Ions

With the two neutral particle analyzers installed in ASDEX Upgrade it is possible to measure simultaneously the fluxes of ripple-trapped ions and banana ions for the different confinement modes as a function of energy. Figure 12 shows the fluxes in L-mode (full line), in H-mode with type III ELMs (dotted line), in ELM-free H-mode (dashed line) and in H-mode with type I ELMs (dash-dotted line) for ripple-trapped ions (left plot) and banana ions (right plot). Fluxes at

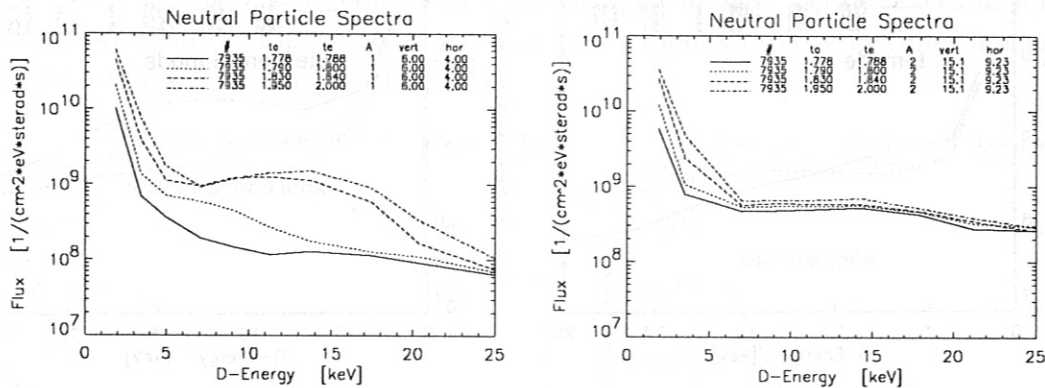


Figure 12: Neutral particle spectra for ripple-trapped (left) and banana (right) ions for different modes of the plasma. Full line: L-mode; dotted: H-mode with type III ELMs; dashed: quiescent H-mode; dash-dotted: H-mode with type I ELMs.

energies below about 5 keV are dominated by thermal plasma ions, and above this energy by slowing down ripple-trapped ions. After L/H-transition fluxes of these latter ions (left plot) increase in time in certain energy ranges, and higher energies are affected with growing radial electric field according to the development of the H-mode. On the contrary the fluxes of banana ions (right plot) grow only very slightly in time, maybe due to changes in the neutral background density, or due to an increase in electron temperature. Thermal ions below 5 keV show

similar behaviour for ripple-trapped and banana ions. The fluxes in Figure 12 are time integrated. As the fluxes during ELMs are low and as the duration of type III ELMs is not negligible compared to the time between Elms, the fluxes of neutrals from ripple-trapped ions for the H-mode with type III Elms could be almost twice as high, if only times between ELMs would have been measured.

In the left and right plots of Figure 13 the fluxes of L-mode and H-mode are compared for different toroidal viewing angles of the analyzer, that is for different pitch angles of the ions. The full line with a horizontal angle of 3.18° represents ripple-trapped ions, the dashed line banana ions, and the dotted line also banana ions very close to the border line to the ripple-trapped ions. In L-mode, for large energies the fluxes of the ripple-trapped ions are well below the fluxes of the banana ions indicating the fast losses due to the gradB-drift. Whether the increase in the flux of ripple-trapped ions towards lower energies is due to increasing collisionality or to a field of a few kV/m during L-mode, is not easy to decide. Details depending on the viewing angle may also play a role and may be understood after more realistic Monte Carlo calculations.

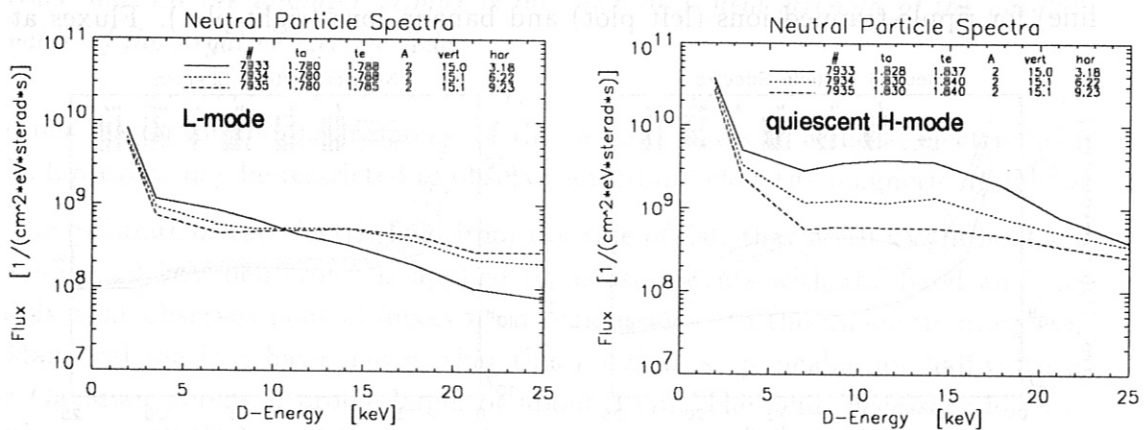


Figure 13: Neutral particle spectra during L-mode (left) and quiescent H-mode (right) for different types of ions. Full line: ripple-trapped; dotted: mixed ripple-trapped/banana; dashed: banana ions.

During quiescent H-mode, right plot in Figure 13, the spectrum of the ripple-trapped ions, (full line), looks quite different from the corresponding L-mode spectrum, whereas the ones for banana ions (dashed lines), are very similar. The radial electric field changes the density of the ripple-trapped ions, but not of the banana ions. This figure is taken with the movable analyzer observing the plasma from below the midplane. As stated in the discussion of Figure 11, orbits of more energetic ions can be influenced by the same field with this viewing angle

than for the viewing angle of the fixed analyzer. This may explain the larger flux of the ripple-trapped ions (full line in left plot of Figure 13) at low energies compared to the flux of banana ions (dashed line), if a small field of a few kV/m is present during L-mode, and may explain the large difference in the flux at 25 keV between L-mode and quiescent H-mode (full lines in left and right plot of Figure 13), although the fluxes in the fixed analyzer suggest a field strength of less or about 20 kV/m. The density of banana ions close to the border line to ripple-trapped ions is influenced by the density of the ripple-trapping region. A more careful measurement near the border line is necessary and possible, in order to determine the influence of the ripple loss cone on the near banana orbits.

The spectra in Figure 14 are taken during H-mode with type I ELMs, left plot for ripple-trapped ions (#7643, 3.4 to 3.6 s, movable analyzer), right plot for banana ions in a similar discharge (#7636, 3.4 to 3.6 s, movable analyzer). The dotted curve is the spectrum, when fluxes are collected only inbetween ELMs, the full curve is the spectrum, when fluxes are collected only during ELMs. The effect of the radial electric field is rather large. The spectrum during ELMs is very similar to the spectrum during L-mode and indicates that the radial electric field during the ELM is drastically reduced or even changed in sign. Time traces of fluxes (see, for example, Figure 16) show that this happens rapidly in times less than 100 μ s at the beginning of the ELM.

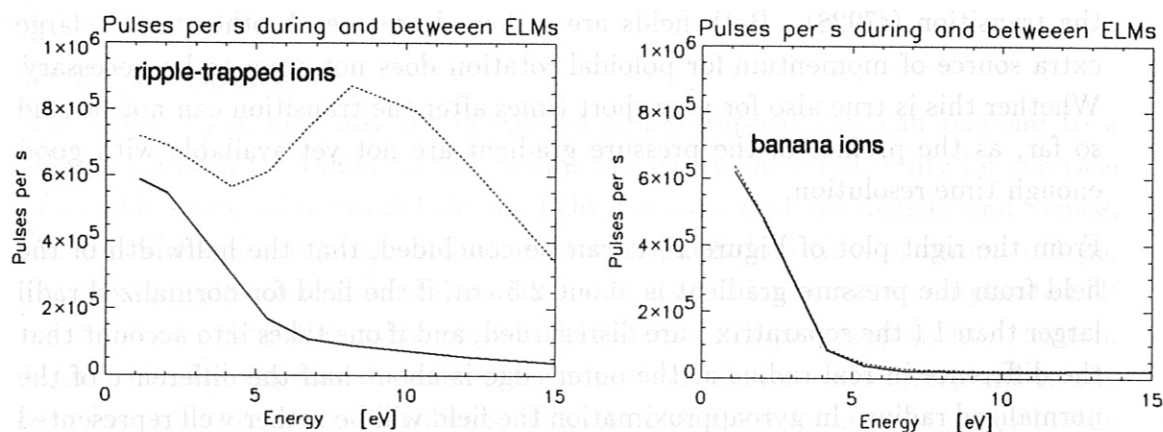


Figure 14: Neutral particle spectra for ripple-trapped (left) and banana (right) ions. Full line: during type I ELMs; dotted: inbetween type I ELMs.

The right plot of Figure 14 shows the spectra, measured with the movable analyzer looking at a toroidal angle of 12° , that is at banana ions, and taken at times inbetween and during the ELMs (times are measured by the other analyzer, looking at ripple-trapped fluxes, which shows the effect of ELMs). There is

almost no difference between the two spectra. Banana ions do not feel ELMs. It can be concluded, that the ELMs do not throw out the energetic ions from neutral injection, but only reduce the radial electric field and allow the ripple-trapped ions to be lost by gradB-drift.

Also at a toroidal angle of 9° the analyzer should see only banana ions; for this pitch angle, which is close to the pitch angle of the ripple-trapped ions, a small change in the spectrum of the banana ions of about 50 percent can be seen. This indicates, that there is a small backscattering from ripple-trapped ions to banana ions, which is especially effective at the border line between the two ion groups and hence the banana ion density very close to the border line is affected by the loss of the ripple-trapped ions.

In Figure 15 an attempt is made to compare the fields estimated from the neutral fluxes with those obtained from pressure gradient. The figure has already been published previously [15]. It is taken from different, but very similar discharges of the same series. The left plot of Figure 15 gives neutral particle spectra measured with the fixed analyzer 10 ms before and 7.5 / 27.5 / 50.0 / 112.5 ms after the L/H-transition, and indicates in the vertical bars an estimate of the maximal value of the radial electric field (the field in kV/m corresponds to the energy in keV). The right plot of Figure 15 shows the electric field from $1/n \cdot \nabla_r p$ for similar times : the curve marked L is before, the other curves are 10 / 50 / 90 ms after the transition (#7928). Both fields are rather close to each other, and a large extra source of momentum for poloidal rotation does not seem to be necessary. Whether this is true also for very short times after the transition can not be said so far, as the profiles of the pressure gradient are not yet available with good enough time resolution.

From the right plot of Figure 15 it can be concluded, that the halfwidth of the field from the pressure gradient is about 2.5 cm, if the field for normalized radii larger than 1 (the separatrix) are disregarded, and if one takes into account that the difference in real radius at the outer edge is about half the difference of the normalized radius. In gyroapproximation the field will be rather well represented by a field with a halfwidth of 3 cm.

4.2 Time dependence of fluxes at the L/H-transition

a) Time resolution

The maximum countrate of the detectors in the neutral particle analyzers is about 1 million per s with negligible saturation effects. A time resolution of 100 μ s affords to operate the interesting channels of the analyzer close to saturation.

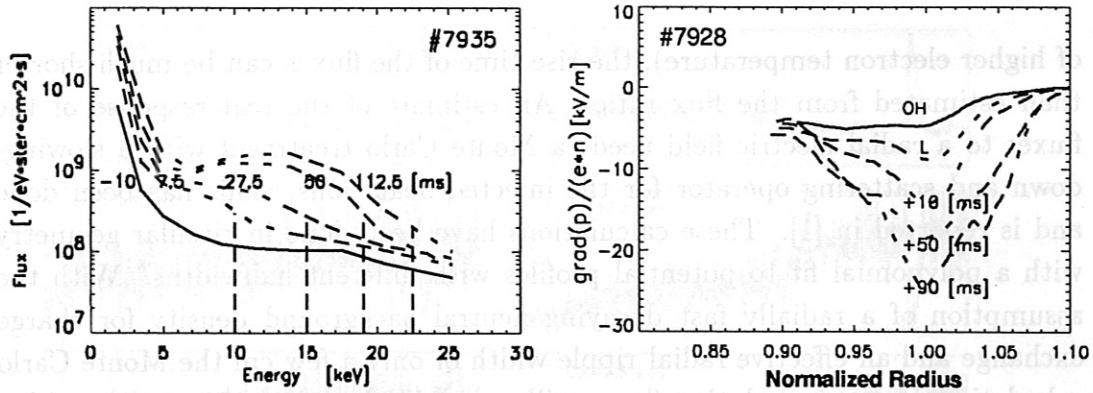


Figure 15: Left: *neutral particle spectra at different times during an L/H-transition with vertical dashed lines that estimate the energy, till which the fluxes are influenced by the electric field.* Right: *Electric field profiles from pressure gradient at different times during an L/H-transition.*

There are two methods available to influence the fluxes at the detector for a given plasma: The first one is offered by the analyzer itself. The pressure in the stripping cell [9] can be varied to change the fraction of the incoming neutrals, that are ionized and detected in the analyzer. The second method uses a local increase of the neutral background density in the observed plasma region by a local gas pulse. Both methods have been applied to optimize the flux of neutrals in the interesting energy range.

b) Time response

The question, of how fast the density of ripple-trapped ions can respond to a sudden jump in the radial electric field is not easily answered. Only for the case of a sudden drop of the radial electric field it is clear that the density and, hence, the fluxes should respond with at least the gradB loss time of about $100 \mu\text{s}$. For the opposite case of a sudden increase the situation is more complicated. If orbits, confined by the radial electric field, remain ripple-trapped, like those in Figure 10, one expects that the rise time of the fluxes will correspond to the new loss time of the confined ions. The ratio of the loss times is given by the ratio of the fluxes. As the fluxes increase by about an order of magnitude and the gradB loss time is about $100 \mu\text{s}$, the new loss time and, hence, the rise time of the fluxes after a sudden increase of the radial electric field should be of the order of 1 ms, if the filling rate of the loss cone is unchanged in both cases. If, however, the radial electric field connects closed or open orbits through the observation point to plasma areas further inside, where the filling rate is much larger, because of smaller ripple and higher slowing-down density (effect

of higher electron temperature), the rise time of the fluxes can be much shorter than estimated from the flux ratio. An estimate of the real response of the fluxes to a radial electric field needs a Monte Carlo treatment with a slowing-down and scattering operator for the injected beam ions. This has been done and is reported in [1]. These calculations have been done in circular geometry with a polynomial fit to potential profiles with different halfwidths. With the assumption of a radially fast decaying neutral background density for charge exchange and an effective radial ripple width of only a few cm the Monte Carlo calculation demonstrated, that fluxes will respond in less than $100 \mu\text{s}$ to a sudden increase of a radial electric field. This picture has been further confirmed with 3D Fokker-Planck calculations [2], where the ripple-trapped, the banana and the passing ion distributions were solved self-consistently with the given neutral beam injection parameters. The ripple-trapped ion distribution was solved in time, space and velocity along practically all possible ripple ion drift orbits in the presence of an abrupt change of the radial electric field. The loss region of the ripple-trapped ions was found to be rapidly ($< 100 \mu\text{s}$) filled by the fast connection of the ripple-trapped ions from the well-filled regions further inside the plasma after an onset of a sufficiently large and wide radial electric field. The dependance of the charge exchange flux on particle energy, electric field width and strength by the onset of the radial electric field was investigated. For a halfwidth of the electric field of less than about the gyro diameter the results are still a bit doubtful, as in the gyroapproximation of the Monte Carlo treatment the applied potential profiles and the corresponding radial electric fields do not seem to be the best representation of the expected real field profile especially for slowing-down ions with their diminishing Larmor radius.

If the radial electric field drops fast, the fluxes undoubtedly will respond at least with the gradB loss time of about $100 \mu\text{s}$.

c) Flux measurements at L/H- and H/L-transitions

Fluxes have been measured with fast time resolution for L/H-transitions with negative and positive toroidal magnetic fields (gradB-drift towards and away from the X-point), and for an H/L-transition with positive toroidal magnetic field. Figure 16 shows the D_α -signal from the divertor region and fluxes for six different energies around an L/H-transition, marked in the figure with a vertical line (#7934 fixed analyzer).

With the drift towards the X-point the plasma transits from L-mode to an H-mode with type III ELMs. As the power across the separatrix continues to increase after the L/H-transition, after a phase with rather constant frequency the ELM frequency reduces, and finally a quiescent H-mode appears. This is

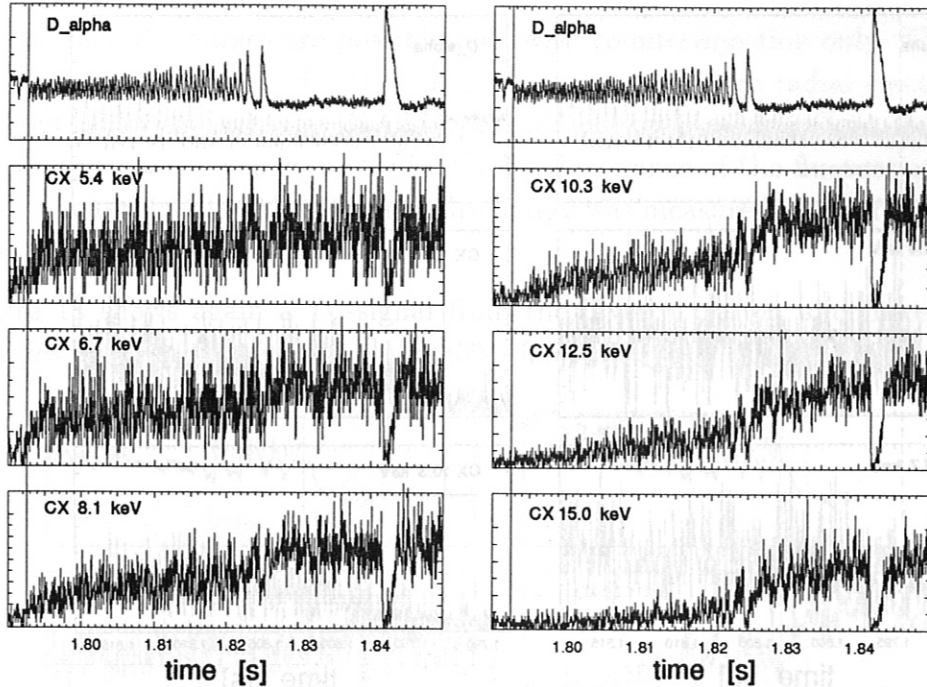


Figure 16: D_α and neutral particle fluxes for different energies during an L/H-transition, marked by a vertical line. An H-mode with type III ELMs is followed by a quiescent phase, which is interrupted by a type I ELM.

interrupted by a type I ELM. Most discharges in ASDEX Upgrade are run with negative toroidal field and experience the described sequence of events. The charge exchange fluxes are measured with a $50 \mu\text{s}$ time resolution. The increase of the fluxes after the L/H-transition occurs the later the higher the energy of the fluxes. At the transition to the quiescent H-mode for the fluxes between 10.3 and 15 keV the rise of the fluxes is accelerated during a few ms. The type I ELM reduces the fluxes to at least L-mode level in less than $100 \mu\text{s}$ for energies above 10 keV and somewhat slower for energies below 10 keV, as is expected from the gradB-drift time. The time to recover from the type I ELM increases from 1.5 ms at 5.4 keV to more than 2 ms at 15 keV.

Even the last low frequency type III ELMs do not seem to reduce the field to L-mode level and the recovery time after a type III ELM seems to be much faster than the increase after the L/H-transition or after a type I ELM. The type III ELM apparently does not destroy the density and temperature profile and the radial electric field as rigorously as a type I ELM.

Figure 17 displays the data for the same discharge on an expanded time scale for the lowest four energies of the fluxes.

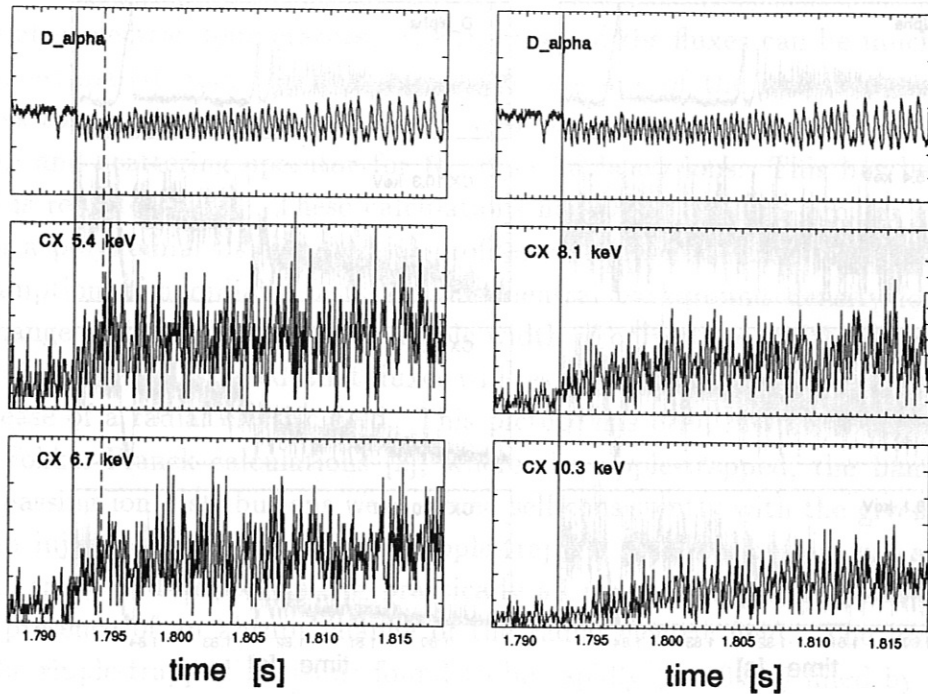


Figure 17: D_α and neutral particle fluxes. The flux at 5.4 keV needs about 2 ms to reach its full value (indicated by the dashed line).

Again the full line marks the L/H-transition. The dotted line for 5.4 keV marks the time at which the flux has reached a constant average level. The rise time to this average flux is 2 ms. As the flux after a type III ELM can apparently increase on a shorter time scale, it is concluded that this slow rise time of the flux is an indication of a slow increase of the radial electric field. This slow rise time of about 2 ms, and the even slower rise time of about 10 ms for the 10.3 keV flux, are far longer than the time, the fluxes would need to respond to a radial electric field. If the halfwidth of the field is larger or about 2 cm, the flux pattern suggests that after the L/H-transition the electric field increases to about 6 kV/m in 2 ms, reaches about 8 kV/m during the type III ELMs, grows to about 10 kV/m in 2 ms after the transition to the quiescent H-mode, and finally reaches 15 kV/m during H-mode with type I ELMs. The values of the field, quoted here, may be quite different in different discharges with different injection powers, magnetic fields or plasma densities. But the sequence of events, as described here, has been observed in a large number of experiments. In particular no increase of the fluxes is observed before the L/H-transition.

With positive toroidal magnetic field and gradB-drift away from the X-point, the plasma transits from L-mode directly to the quiescent H-mode. For technical

reasons such discharges are possible now with counterinjection only. These discharges have the peculiarity that they develop rather large radial electric fields of about 10 kV/m and type III ELMs already during L-mode [16], at least, if the transition time is given correctly by the disappearance of the fluctuations in the reflectometer signal, which for these discharges was measured with an uncertainty of ± 0.5 ms [17].

Figure 18 shows again a D_α -signal from the divertor region and fluxes for six energies between 10.8 and 30 keV (#8594, fixed analyzer). The transition time at

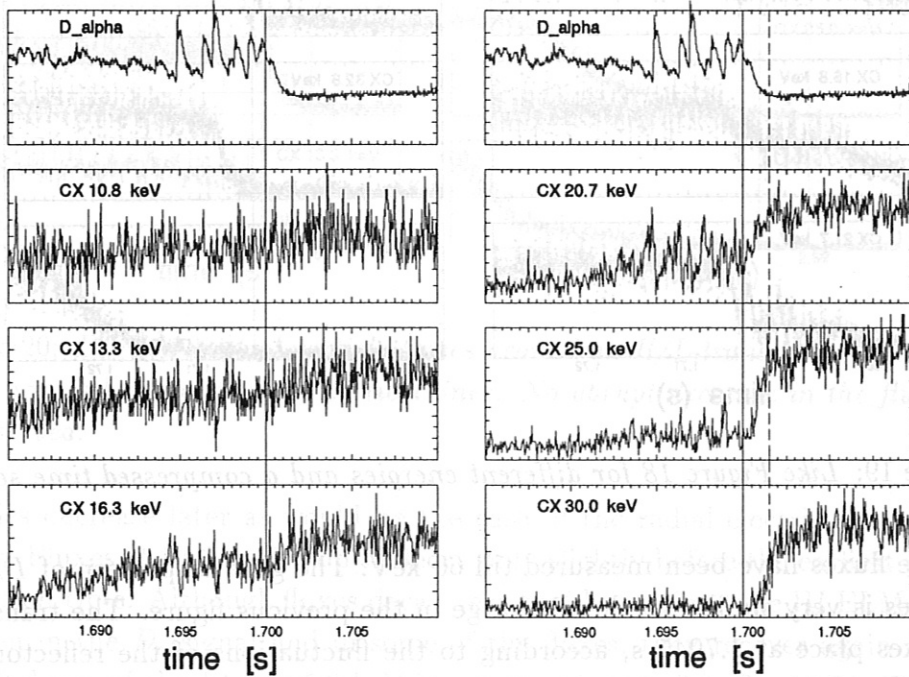


Figure 18: D_α and neutral particle fluxes for gradB-drift away from the X-point and counterinjection around the L/H-transition, marked by a vertical line. The fluxes need about 1.5 ms to reach their full value.

1.7 s is marked by a solid vertical line. Fluxes at 10.8 and 13.3 keV show little influence of ELMs or the transition: Ions of these energies are already confined, that is, the radial electric field may be as high as 13 kV/m and remain so during the ELMs. Fluxes at 20.7 keV increase before the ELMs to almost their constant post-transition value, indicating, that the radial electric field increases to almost 20 kV/m before the ELMs. Fluxes at 25 and 30 keV experience a larger increase only after the L/H-transition. This increase of the fluxes after the transition takes place in about 1.5 ms and starts the later, the higher the energy.

A second discharge (#8595 fixed analyzer) with positive toroidal magnetic field

(Figure 19) was investigated with a high time resolution of $50 \mu\text{s}$, in this case slightly smoothed with $30 \mu\text{s}$ (points mark the original data).

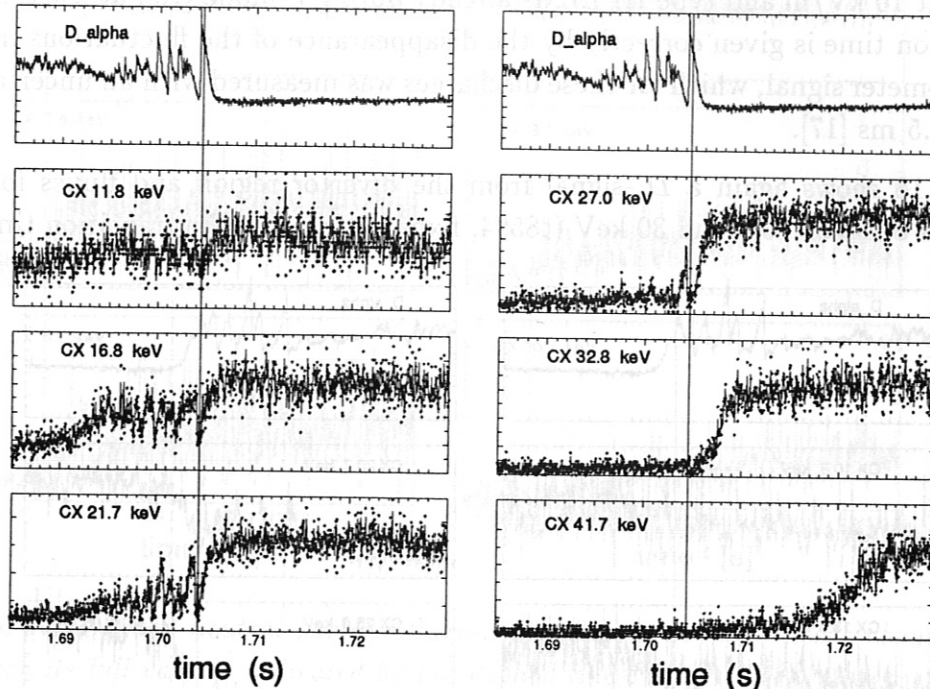


Figure 19: Like Figure 18 for different energies and a compressed time scale.

Here the fluxes have been measured till 60 keV. The general pattern of D_α and the fluxes is very similar to the discharge in the previous figure. The transition here takes place at 1.7045 s, according to the fluctuations of the reflectometer signal. The field seems to increase from about 12 kV/m up to about 25 kV/m before the last ELM, then to about 30 kV/m in 1.5 ms after the transition to the quiescent H-mode. In later times the field continues to grow on an even slower time scale. Even fluxes of 50 keV ions (not shown on the figure) increase later than 20 ms after the transition, indicating, that radial electric fields of at least 40 kV/m have been obtained.

Figure 20 (#8572 fixed analyzer) is the only example of an H/L-transition with a fast time resolution of $100 \mu\text{s}$. For this discharge with positive toroidal field the reflectometer diagnostic did not register the fluctuations and therefore there is no good marker for the H/L-transition available. The transition takes place during the strong increase of the D_α -signal. It is caused by volume radiation due to an impurity event.

Fluxes at 30 keV start to decrease already 30 ms before the transition, lower

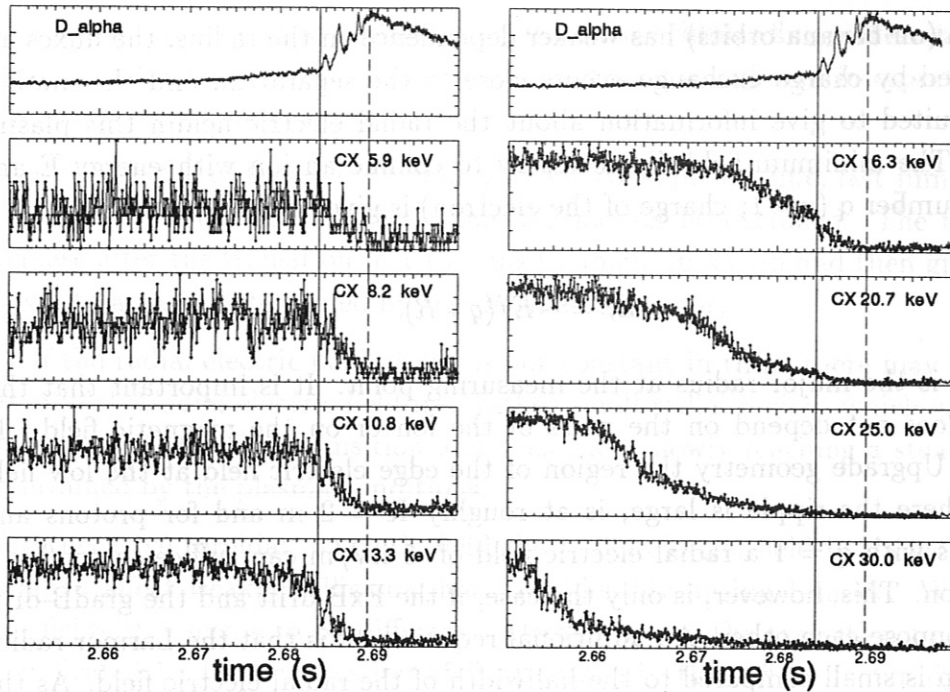


Figure 20: D_α and neutral particle fluxes around an H/L-transition. The time of transition is between the two vertical lines. No abrupt decrease in the fluxes can be observed.

energies decrease later as would be the case, if the radial electric field decayed slowly. Fluxes at 13.3 keV start to decay only slightly before the earliest possible transition time. Although fluxes decay very rapidly during type III ELMs as can be seen in the D_α -signal and in some of the fluxes, they recover again and the overall decay of the 13.3 to 5.8 keV ions takes place in 2 to 3 ms. The loss time for confined ripple-trapped ions in this case is definitely of the order of 100 μ s.

5 Conclusions and summary

The density of energetic, that is weakly collisional ions that are trapped in the magnetic ripples due to the discrete toroidal field coils, depends sensitively on the presence of a radial electric field in the plasma edge. As the here described method, to measure this density, uses charge exchange, the measured signal is dominated by fluxes from plasma regions, where the product of ion density and neutral background density is large. As the neutral density decays almost exponentially at the plasma edge, but the density of injected ions from neutral

injection (on banana orbits) has weaker dependence on the radius, the fluxes are dominated by charge exchange events close to the separatrix, and the method is well suited to give information about the radial electric field in this plasma region. The minimum field E_r necessary to confine an ion with energy E and charge number q ($q=-1$: charge of the electron) is given by

$$E_r = -E/(q * R)$$

where R is the major radius at the measuring point. It is important that this energy does not depend on the mass of the ion or on the magnetic field. In ASDEX Upgrade geometry the region of the edge electric field at the low field side, where the ripple is large, is at roughly $R = 2$ m and for protons and deuterons with $q = 1$ a radial electric field of -5 kV/m can suffice to confine a 10 keV ion. This, however, is only the case, if the ExB-drift and the gradB-drift exactly oppose each other. An additional requirement is that the Larmor radius of the ion is small compared to the halfwidth of the radial electric field. As the Larmor radius of a 10 keV deuteron in a 2 T field is about 1 cm, the ExB-drift is reduced in a radial electric field with a halfwidth of only a few cm; with a halfwidth of 1 cm in a Gaussian potential profile the reduction is already a factor of 2; for a halfwidth of 2 cm the reduction is only 20 %. Since from the size in the gradient zone at the plasma edge a halfwidth of about 2.5 cm is expected in ASDEX Upgrade (see Figure 15), it has been assumed in this paper as a rough estimate of the radial electric field that a field of -10 kV/m can confine 10 keV deuterons. For magnetic fields lower than 2 T or a halfwidth of the radial electric field less than 2 cm the necessary field strength will be larger.

Banana ions far enough from the ripple-banana boundary are not influenced by the radial electric field. Their fluxes are indeed constant also during ELMs. Also fluxes of ripple-trapped ions with energies larger than can be affected by the electric field are not influenced by the ELMs. It can be concluded, that ELMs do not remove the edge fast ions from the plasma. A thorough investigation, how much banana ions close to the banana-ripple boundary are affected, has not yet been done. But even a 3 ° toroidal deviation of the analyzer from the near optimum observation of ripple-trapped ions to a position close to the boundary reduces the flux and the influence of the radial electric field on the ions considerably.

The statements in this paper about the radial electric field and the time behaviour are made under the assumption, that the profile during the L/H- and the H/L-transition stays constant with a halfwidth of the field of about 2 cm or more. If the radial electric field starts to grow in regions much smaller than 2 cm and expands

in course of time, this will probably produce a very similar flux pattern to the one observed if the fields are large enough. Therefore, two different interpretations of the flux patterns are possible:

1.) If the profile of the electric field is about constant in time, fast jumps in the radial electric field in times less than $200 \mu\text{s}$ can be excluded. The field may increase after the transition in 1 to 2 ms to about 10 kV/m and then grow more slowly to a value determined by the plasma conditions.

2.) If the radial electric field profile is not constant in time, there may be a fast jump in the radial electric field in a rather small radial region, which grows fast during 1 to 2 ms after transition and then more slowly reaching a steady state, determined by the plasma conditions.

With negative toroidal magnetic field the radial electric field in the edge is too small to affect weakly collisional ions considerably during L-mode. With positive fields this seems to be different. Already before the transition to H-mode, as indicated by the suppression of fluctuations in the reflectometer signal, the radial electric field reaches values of about 20 kV/m and shows a strong increase before transition. On the other hand, the transition seems to take place after an ELM, when the radial electric field is almost zero. It could be imagined, that fluctuation measurement with better time resolution would show, that the plasma already undergoes short transitions to H-mode before each ELM. Under such circumstances the measurements reported here would not be in contradiction to the earlier statement [8], that the electric field increases only after the L/H-transition. But at present it can not be excluded that with positive toroidal magnetic field (and counterinjection), that is, with gradB-drift away from the X-point, rather large radial electric fields exist already during L-mode. As this L-mode phase is characterized by type III ELMs and an improved confinement [16], a careful examination of the fluctuation should be performed to verify the real status of this phase of the discharge.

That the radial electric fields are so large in the case of counterinjection may be interpreted [15] as the contribution to the field from toroidal rotation caused by neutral injection, which with counterinjection has the same sign as the field from pressure gradient, whereas the sign is opposite for coinjection. It could very well be, that the field from the toroidal rotation has a small gradient and does contribute little to the suppression of fluctuations.

6 Acknowledgements

Thanks go to H.-U. Fahrbach for his competent operation of the charge exchange analyzers and to M. Kaufmann, K. Lackner, A. Peeters, W. Suttrop, F. Ryter from IPP, H. Zohm from IPF Stuttgart, for valuable discussions and suggestions. The continuous discussion and exchange of ideas with J. Heikkinen from VTT Helsinki, Finland, and T. Kurki-Suonio from HUT, Helsinki, Finland, has been of large benefit for this work and I am very grateful to them. Data and work of the following colleagues have been used and their support is especially acknowledged: B. Kurzan for fluctuation measurements of the reflectometer; J. Stober for the evaluation of the neutral density profile; Cl. Hofmann for the approximate formula to describe the ripple in ASDEX Upgrade; W. Schneider for his programs to calculate the magnetic field and related quantities; O. Gehre, J. Schweinzer, Ch. Fuchs for plasma density profiles; H. Murmann, H. Salzmann for the Yag electron temperature profiles.

7 References

- [1] J. A. Heikkinen, W. Herrmann, T. Kurki-Suonio, Phys of Plasmas 4 (1997) 3665
- [2] J. A. Heikkinen, T. Kurki-Suonio, "Analysis of the Tokamak ripple-blocked ion distribution with abrupt changes of a radial electric field", accepted for publication by Phys of Plasmas
- [3] K. Itoh and S.-I. Itoh, Plasma Physics and Controlled Fusion, 38, 1 (1996)
- [4] W. Herrmann, 17th EPS Conf. on Controlled Fusion and Plasma Heating, Amsterdam (1990), Vol.4, p.1672
- [5] M. C. Zarnstorf et al., Physics of Plasmas, 4, 1097, (1997)
- [6] V. Rohde et al., J. Nucl. Mat. 241-243 (1997) p. 712
- [7] K. H. Burrell et al., Laboratory Report GA-A22185 (1995): Constraints on theories provided by fast time response E_r measurements across the L to H transition on DIII-D.
- [8] W. Herrmann and ASDEX Upgrade Team, Phys. Rev. Letters, 75, 4401 (1995)
- [9] R. Bartiromo et al., Rev.Sci.Instrum.,58,(1987),788
- [10] Cl. Hofmann, unpublished
- [11] J. Stober and ASDEX Upgrade Team, Plasma Phys. Control. Fusion 39

(1997) 1145

[12] D. Reiter, KFA Juelich reports, JueL-1947,(1984),Juel-2599,(1992)

[13] W. Ott, E. Speth, A. Staebler IPP-Report 4/161 (1977)

[14] P. J. McCarthy, W. Schneider et al., 1992 Int. Conf. on Plasma Physics, and 19th EPS Conf. on Controlled Fusion and Plasma Heating, Vol 16C, Part 1, page I-142

[15] H. Zohm et al., 16th IAEA Fusion Energy Conf., Montreal 1996

[16] F. Ryter et al., H-mode workshop Seeon, Germany, (1997), to be published in a special issue of Plasma Physics and Controlled Fusion.

[17] A. Silva et al., Rev. Sci. Instrum. 67 (1996) 4138